



Seismicity and one-dimensional velocity structure of the Himalayan collision zone: Earthquakes in the crust and upper mantle

G. Monsalve,¹ A. Sheehan,¹ V. Schulte-Pelkum,¹ S. Rajaure,² M. R. Pandey,² and F. Wu³

Received 21 September 2005; revised 7 April 2006; accepted 9 June 2006; published 3 October 2006.

[1] Earthquakes beneath the Himalayan collision zone occur at depths between near surface and around 100 km below sea level. After relocating earthquakes with two one-dimensional (1-D) velocity models, we found a clear bimodal depth distribution for earthquakes in the Himalayas of eastern Nepal and the southern Tibetan Plateau and evidence that some earthquakes originate at upper mantle depths. Seismicity in Nepal shows an accumulation of earthquakes along the front of the Himalayan arc, with a seismic gap between longitudes 87.3°E and 87.7°E. Although upper crustal seismicity along the topographic front of the High Himalaya is consistent with a region of high strain accumulation associated with convergence on the Main Himalayan thrust fault, microearthquakes do not necessarily occur on this fault. Instead, they concentrate in the hanging wall. Seismic activity in the sub-Himalaya and the Terai Plains is almost exclusively limited to the vicinity of the location of the magnitude 6.5 20 August 1988 Udayapur earthquake, with most of the earthquakes in the lower crust and the upper mantle. Clusters of earthquakes in the Lesser and High Himalayas and south Tibet (Tethyan Himalayas) mark very well defined zones of seismicity at depths between 50 and 100 km, confirming the presence of earthquakes in the upper mantle in the region of continental collision. The occurrence of earthquakes at sub-Moho depths favors the idea that the continental upper mantle deforms by brittle processes.

Citation: Monsalve, G., A. Sheehan, V. Schulte-Pelkum, S. Rajaure, M. R. Pandey, and F. Wu (2006), Seismicity and one-dimensional velocity structure of the Himalayan collision zone: Earthquakes in the crust and upper mantle, *J. Geophys. Res.*, *111*, B10301, doi:10.1029/2005JB004062.

1. Introduction

[2] The Indian Plate underthrusts the Himalayas and south Tibet in a NNE direction. The top of the underthrusting Indian Plate has been interpreted to coincide with the Main Himalayan thrust fault (MHT) [Nelson, 1996], which is accommodating most of the relative motion between India and Tibet [Lave and Avouac, 2000]. Since there is an absence of historical earthquakes in several portions of the Himalayan arc, there is potential energy available to generate large earthquakes ($M > 8$) [Jouanne *et al.*, 2004].

[3] It is known that seismic events cluster along the Himalayan arc in a narrow zone, nearly 50 km wide, just south of the Main Central Thrust [Ni and Barazangi, 1984]. Slip during these earthquakes on the Himalayan front contributes to underthrusting on the Main Himalayan thrust fault and are crucial for evaluation of plausible geometries

of this major structure, as well as locked portions of the fault and areas where stress and strain accumulate during the interseismic period.

[4] One of the main characteristics of the seismicity in southern Tibet is the occurrence of earthquakes at upper crustal depths [Langin *et al.*, 2003]. The presence of intermediate depth earthquakes (depths between 70 and 100 km), possibly in the upper mantle beneath southern Tibet and the High Himalayas, has been documented by several authors [Chen *et al.*, 1981; Molnar and Chen, 1983; Chen and Molnar, 1983; Zhao and Helmberger, 1991; Zhu and Helmberger, 1996; Langin *et al.*, 2003; Chen and Yang, 2004; Kayal, 2001]. Pandey *et al.* [1999] suggest an upper mantle location for the 20 August 1988 local magnitude 6.5 Udayapur earthquake beneath the Lesser Himalaya of Nepal. There is a controversy on whether all these deep earthquakes are in the lower crust or in the uppermost mantle. Jackson [2002], Maggi *et al.* [2000a], and Mitra *et al.* [2005] argue that all the earthquakes beneath the Himalayas and south Tibet are in the crust, which is extremely thick in this part of the world. On the other hand, Zhu and Helmberger [1996] and Chen and Yang [2004] present evidence of earthquakes from this region with upper mantle origin.

¹Department of Geological Sciences and CIRES, University of Colorado, Boulder, Colorado, USA.

²Department of Mines and Geology, National Seismological Centre, Kathmandu, Nepal.

³Department of Geological Sciences and Environmental Studies, State University of New York at Binghamton, Binghamton, New York, USA.

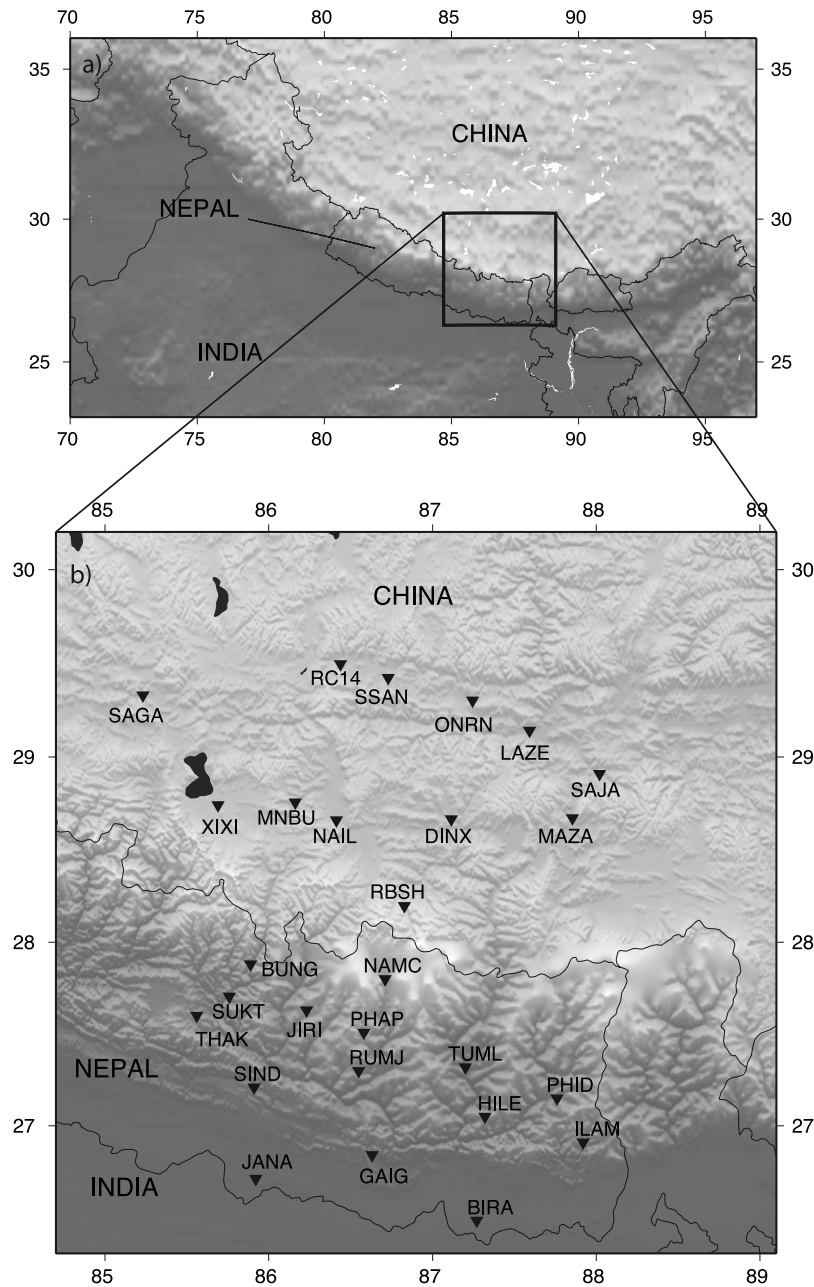


Figure 1. (a) Overview map with the topography of an area of central Asia. Black rectangle outlines the study area. (b) Topography of the study area and HIMNT broadband seismic 2001–2003 station network. Inverted triangles represent locations of PASSCAL broadband seismic stations. A four-letter code for each station is shown.

[5] In this paper we summarize the process to obtain local earthquake locations from a temporary seismic network in eastern Nepal and southern Tibet, and discuss some of the implications of the obtained seismicity, with special emphasis on the location of the intermediate depth earthquakes, in order to address the question on whether these events are in the lower crust or in the upper mantle.

2. Description of the Network

[6] The Himalaya Nepal Tibet Seismic Experiment (HIMNT) consisted of the deployment of a broadband

IRIS-PASSCAL network with 27 Streckeisen STS2 seismometers installed throughout eastern Nepal and southern Tibet with approximately 40–50 km station spacing (Figure 1). The instruments recorded data continuously at rates of 40 and 50 samples per second, between September 2001 and April 2003. The experiment was designed to simultaneously monitor the plains of eastern Nepal, the eastern Himalayas of Nepal and the southern Tibetan Plateau. Table 1 summarizes the station information. A

Table 1. HIMNT Station Network

Station Code	Latitude, deg	Longitude, deg	Elevation, m	Install Date	Removal Date
BIRA	26.484	87.267	12	19 Oct 2001	10 Nov 2002
BUNG	27.877	85.891	1191	13 Oct 2001	6 Apr 2003
GAIG	26.838	86.632	166	14 Oct 2001	3 Jun 2002
HILE	27.048	87.324	2088	12 Oct 2001	6 Nov 2002
ILAM	26.910	87.923	1181	17 Oct 2001	30 Oct 2002
JIRI	27.634	86.230	1866	15 Oct 2001	22 Oct 2002
NAMC	27.803	86.715	3523	21 Oct 2001	31 Mar 2003
PHAP	27.515	86.584	2488	14 Oct 2001	1 Apr 2003
PHID	27.150	87.765	1176	22 Oct 2001	31 Oct 2002
RUMJ	27.304	86.548	1319	10 Oct 2001	3 Apr 2003
SIND	27.211	85.910	465	19 Oct 2001	6 Apr 2003
THAK	27.600	85.557	1551	16 Oct 2001	7 Nov 2002
TUML	27.321	87.195	360	10 Oct 2001	21 Dec 2002
LAZE	29.140	87.592	401	21 Jul 2002	27 Oct 2002
SAJA	28.909	88.021	435	23 Jul 2002	7 Nov 2002
ONRN	29.302	87.244	4350	13 Jul 2002	2 Aug 2002
SSAN	29.424	86.729	4585	14 Sep 2001	8 Sep 2002
SAGA	29.329	85.232	4524	16 Sep 2001	31 Oct 2002
DINX	28.665	87.116	4374	26 Sep 2001	6 Nov 2002
RBSH	28.196	86.828	5100	20 Sep 2001	21 May 2002
NAIL	28.660	86.413	4378	26 Jun 2002	3 Nov 2002
MNBU	28.756	86.161	4500	18 Jul 2002	5 Nov 2002
XIXI	28.741	85.690	4660	15 Jul 2002	1 Nov 2002
RC14	29.497	86.437	4756	14 Jul 2002	28 Oct 2002
MAZA	28.671	87.855	4367	24 Jul 2002	7 Nov 2002
JANA	26.711	85.924	77	13 Nov 2001	5 Feb 2003
SUKT	27.706	85.761	745	5 Mar 2002	7 Nov 2002

more complete description of the experiment and the instrumentation is given by *de la Torre and Sheehan* [2005].

3. Data Processing

[7] We used a set of routines of the Boulder Real Time Technologies (BRTT) ANTELOPE software for automatic detection of first arrivals, manual adjustment of arrival times, preliminary earthquake location and magnitude determination. We use earthquakes reported by the National Seismological Centre at the Department of Mines and Geology (DMG) of Nepal during the time of the experiment in order to contribute with the event detection. We picked first arrival times of P and S waves for seismic events inside the network and assigned a time uncertainty to each arrival; time uncertainties range from 0.05 to 1 s for P wave arrivals and from 0.15 to 2 s for S wave arrivals. Local magnitude was assigned to the earthquakes, ranging from 1 to 5.5. The magnitude determination routine is set up so that the maximum amplitude of the vertical traces within a time window of 90 s is measured for each station recording a specific earthquake. The program determines magnitude for all stations and averages them. The magnitude-frequency distribution of our HIMNT earthquakes indicates that our catalog is complete for magnitudes above 2.5. Comparison with moment magnitudes estimated from full waveform moment tensor inversion for a subset of events [*de la Torre*

et al., 2005] reveals that the moment magnitudes are systematically higher than the local magnitudes by a mean of 0.19 magnitude units.

4. Preliminary Locations

[8] We located a total of 1649 local earthquakes, using a weighted least squares location method with two different three-layer velocity models, one for the Himalayas of Nepal and one for south Tibet. We used the dbloc2 interface to the GENLOC library in the BRTT Antelope package [*Pavlis et al.*, 2004] for earthquake location. All available arrivals were inverted for location. The weight of each arrival is in proportion to the inverse of the length of its uncertainty and is tied to the event-station distance. We located events with four arrivals or more, with at least one S wave arrival, recorded at a minimum of 3 stations.

[9] Since seismic wave speeds vary from south to north across the study area, we used two different velocity models to locate events, one for the Nepal area (Table 2) [*Pandey et al.*, 1999] and another for south Tibet (Table 3) [*Cotte et al.*, 1999]. For earthquakes near the boundary between these two areas, the location was calculated using the model corresponding to the volume through which the majority of rays propagate. Initial locations for 1649 local earthquakes were thus obtained.

Table 2. Velocity Model for Initial Earthquake Locations in Nepal^a

Depth Range, km	P Wave Speed, km/s	S Wave Speed, km/s
Surface to 23	5.6	3.2
23–55	6.5	3.7
>55	8.1	4.6

^aFrom *Pandey et al.* [1995]. Depths are relative to sea level.

Table 3. Velocity Model for Initial Earthquake Locations in South Tibet^a

Depth Range, km	P Wave Speed, km/s	S Wave Speed, km/s
Surface to 40	6.0	3.5
40–70	6.5	3.8
>70	8.1	4.6

^aFrom *Cotte et al.* [1999]. Depths are relative to sea level.

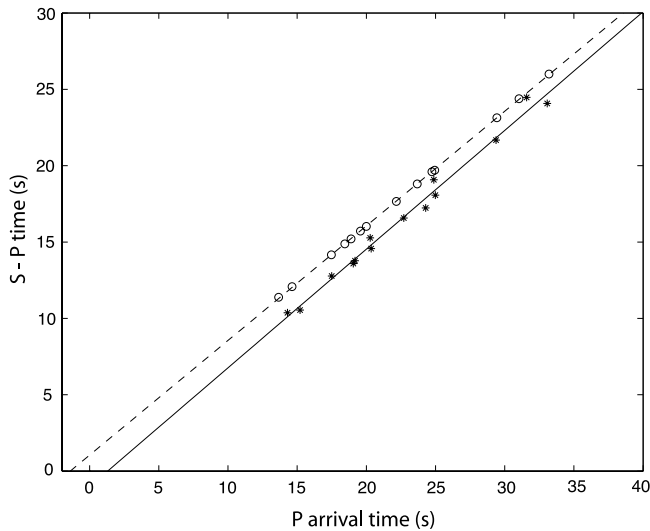


Figure 2. Wadati diagrams for a magnitude 4.17 event in south Tibet (latitude 28.51°N , longitude 86.52°E) occurred on 8 May 2002. Zero time is 1757:00.00. Asterisks denote observed arrivals. Solid line represents the best fit to the observed arrivals in a least squares sense. Circles and dotted line correspond to the predicted arrivals for the best fit location using the a priori three-layer velocity model [Cotte *et al.*, 1999].

[10] In order to get a priori constraints on the velocity model of the study area, we use Wadati diagrams to estimate the average P to S wave speed ratio (V_p/V_s) at several depths and the origin time and its deviation from the time predicted by the preliminary locations. Figure 2 shows two Wadati diagrams for a magnitude 4.17 earthquake in south Tibet, one of them using the observed arrivals, and the other using the predicted arrivals for the best fit solution. From the Wadati diagram we see that the S-P time should be smaller than predicted; this suggests that the true S wave average speed should be faster than in the Cotte *et al.* [1999] model. Observed P arrivals are systematically late with respect to the predicted ones (but in this case the time differences are smaller than 1 s), so the true average P wave velocity should be slightly faster than in the Cotte *et al.* [1999] model. The observed arrivals suggest a V_p/V_s ratio of 1.78 whereas the predicted arrivals give a V_p/V_s ratio of 1.75; the difference in origin time given by both sets of arrivals (intercept with the time axes) is 2.7 s. We made this kind of diagram for all events with 6 or more pairs of P and S arrivals available within the study area and compute the difference in origin time (origin time from predicted arrivals, minus origin time from observed arrivals). Figure 3 illustrates these differences as a function of depth for events in Nepal (Figure 3a) and Tibet (Figure 3b). In particular, for the case of Tibet (Figure 3b), it is clear that the average speeds should be faster than in the Cotte *et al.* [1999] model for events with depths greater than 40 km (origin time should be later than the one predicted by the model, which is the case shown in Figure 2) and slower for events shallower than that. In addition, Wadati diagrams show that

the upper crust in south Tibet (depths shallower than 40 km) has low V_p/V_s values (around 1.66).

5. Improved 1-D Velocity Model and Locations

[11] We used the program VELEST with the method outlined by Kissling *et al.* [1994] to simultaneously invert for earthquake locations, 1-D velocity structure and station corrections, using P and S arrival time data, the initial earthquake locations and a starting velocity model. The inversion is made through a least squares formulation, minimizing the weighted misfit between predicted and observed arrival times. Details of the inversion process are described by Kissling *et al.* [1994].

[12] Given the strong lateral heterogeneity in the study area and the differences in velocity structure between Nepal and Tibet, we divided the area in two regions, north and

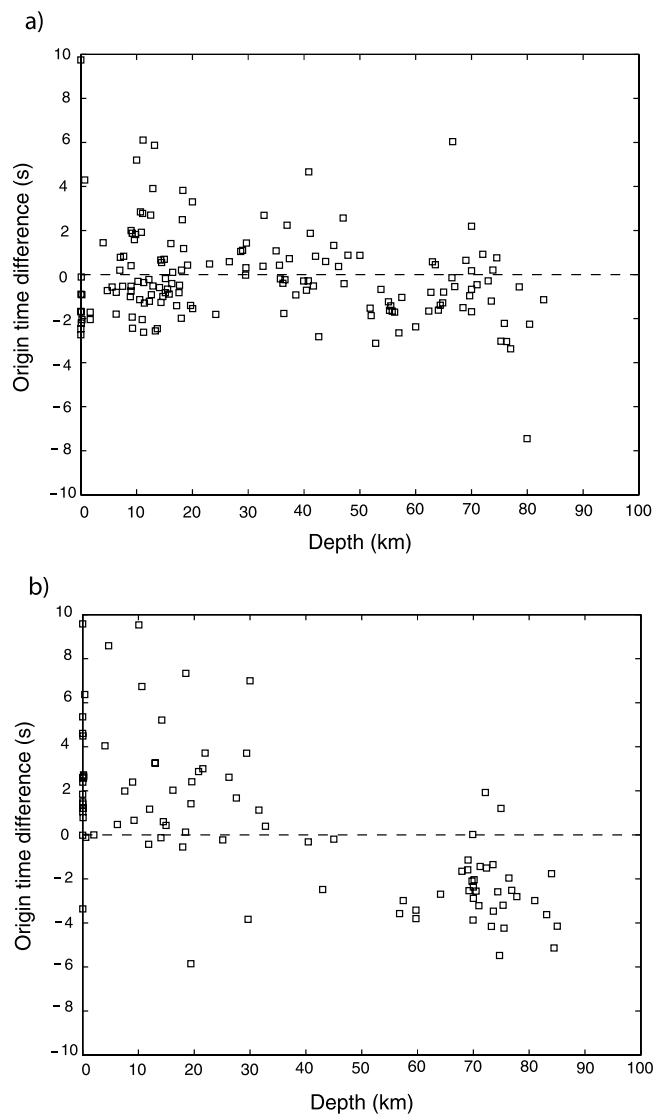


Figure 3. Origin time difference versus depth, computed using Wadati diagrams with observed and predicted arrivals. Only earthquakes with six or more pairs of P and S arrivals recorded at the same station are shown. (a) Events in Nepal. (b) Events in Tibet.

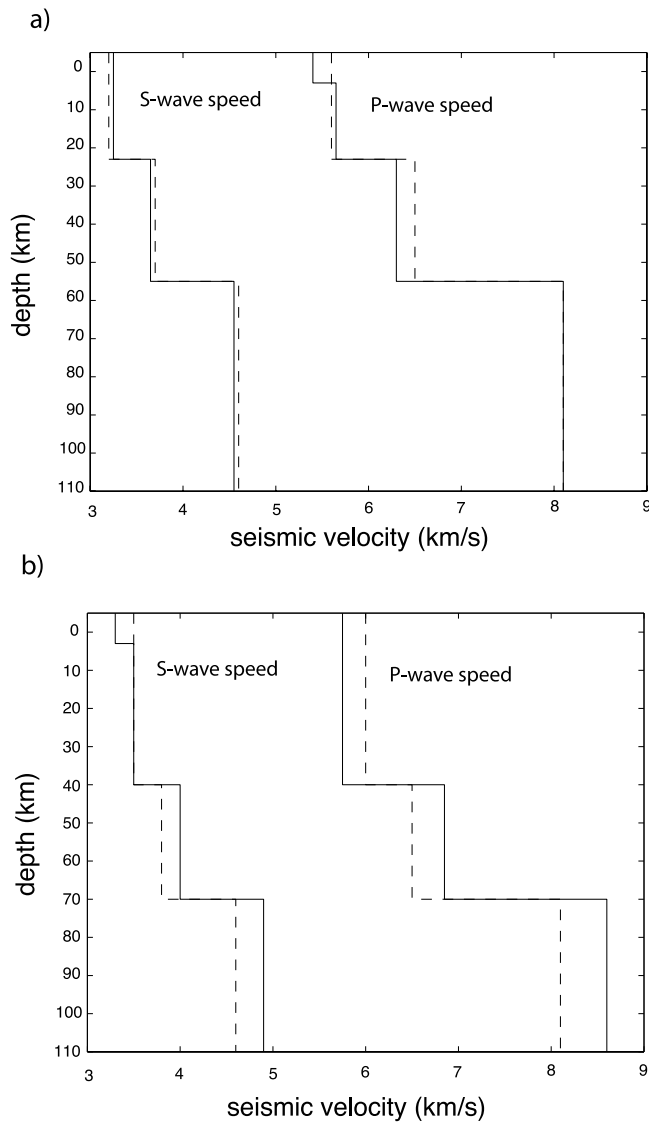


Figure 4. One-dimensional velocity models used for preliminary locations (dashed lines) and the minimum error model found with VELEST (solid lines). (a) Results for the Nepal part of the array. Initial model is by *Pandey et al.* [1995]. (b) Results for the Tibet part of the array. Initial model is by *Cotte et al.* [1999].

south of latitude 28° N. Earthquakes with 7 or more arrivals, recorded at stations within 200 km, with an RMS time residual smaller than 1.5 s at the initial location and longitudes between 85° and 89° E were selected for use in the velocity inversion. A total of 174 earthquakes at latitudes between 28° and 30° N were relocated in the Tibet region and 368 earthquakes at latitudes between 26° and 28° N were relocated in the Nepal region. For the traveltimes inversion, we used 2661 P wave arrivals and 2487 S wave arrivals for the Nepal area, and 1322 P wave arrivals and 1231 S wave arrivals for the Tibet area. We kept the depths of the subsurface layer boundaries fixed at the depths given by *Pandey et al.* [1995] (Table 2) and *Cotte et al.* [1999] (Table 3), and a low-velocity layer, from the surface to a depth of 3 km below sea level, was allowed.

[13] Inversions for earthquake location, P and S wave speeds and station corrections were carried out for the Nepal and Tibet data sets. We searched for a solution on the basis of minimum RMS arrival time residual, making sure that the solutions match the a priori information obtained from initial locations, Wadati diagrams and previous studies [e.g., *Sapin et al.*, 1985; *Pandey et al.*, 1999; *Galvé et al.*, 2002]. Even though we ran the first inversions using the models in Tables 2 and 3 as starting models, we kept changing the starting models in subsequent models, we arrived at solutions with smaller misfits. Random variations of models in Tables 2 and 3 were also used as starting

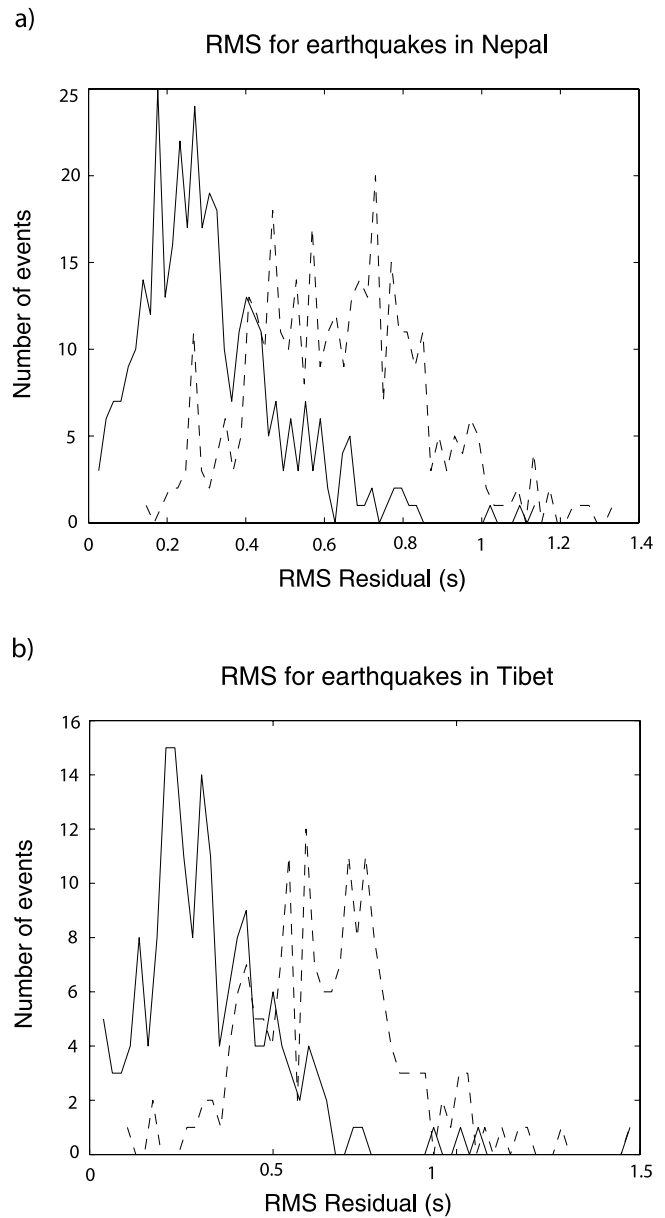


Figure 5. Histograms of RMS misfit for individual events after initial earthquake locations (dashed) and after running VELEST (solid). Only events belonging to the set selected for simultaneous inversion (earthquake location, seismic velocities and station corrections) are used. (a) Results for the Nepal region. (b) Results for the Tibet region.

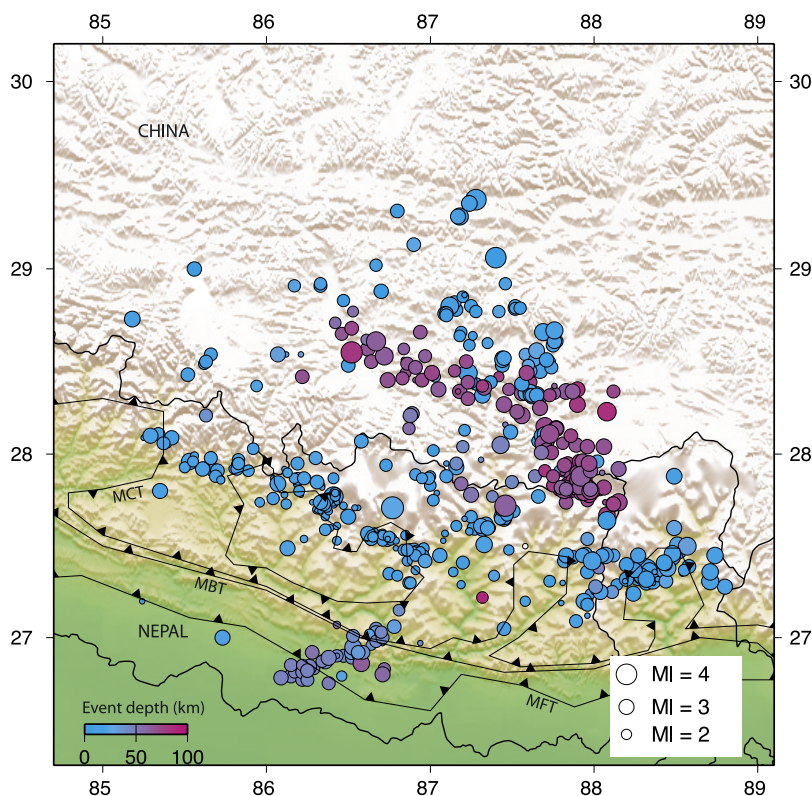


Figure 6. Map view of event relocations for the subset of 542 events selected for inversion using VELEST. Event symbol size is scaled by magnitude. Earthquakes are color-scaled by depth in km. Main Himalayan tectonic structures from *Dasgupta et al.* [2000] and *Lave and Avouac* [2000]. MFT, Main frontal thrust; MBT, Main boundary thrust; MCT, Main Central Thrust.

models in order to perform a better exploration of the parameter space. The velocity models resulting from the traveltimes inversion are shown in Table 4 (Nepal), Table 5 (Tibet), and Figure 4 (solid lines). A dramatic decrease in the RMS arrival time residual for individual events, with respect to the initial locations, can be seen in Figure 5. The total RMS residual went down from 0.751 s before inversion to 0.367 s after inversion for the case of Nepal; in the case of Tibet, it went from 0.954 to 0.381 s. Relocations for this set of earthquakes are shown in Figures 6 (map view) and 7 (arc-normal cross section).

6. Seismicity

[14] Using the new 1-D velocity models (solid lines in Figure 4), the initial 1649 events were independently relocated using the program VELEST [*Kissling et al.*, 1994]. Figures 8 and 9 show these locations in map view and Himalayan arc-normal cross section, respectively. We calculated uncertainties for these locations using 95% confidence intervals. The mean depth uncertainty is 3.5 km and the mean horizontal error is nearly 5.5 km.

[15] Earthquakes in the Himalayas show an alignment on the region of highest relief. Clusters of upper crustal earthquakes on the north part of the network are mostly related to normal faults and grabens in south Tibet [*Langin et al.*, 2003]. Two groups of earthquakes with low crustal and upper mantle depths stand out: a cluster of earthquakes at depths between 30 and 70 km beneath south Nepal, in the

vicinity of the magnitude 6.5 20 August 1988 Udayapur earthquake [*Pandey et al.*, 1999], and a NW-SE stripe of earthquakes at depths between 50 and 100 km beneath south Tibet and the High Himalayas.

[16] The width of the belt of microearthquakes along the topographic front of the High Himalaya (Figure 8) reaches about 70 km at a longitude of 87°E, but in general earthquakes localize within a 50 km width zone, and indicate a zone of stress accumulation during the interseismic period [*Pandey et al.*, 1995]. This might be related with a flat and ramp geometry on the Main Himalayan Thrust Fault. Figure 9 shows that microearthquakes beneath the region of highest relief preferentially locate in the hanging wall, in the overlying thrust sheet, indicating that the possible ramp and southern flat portions of the Main Himalayan thrust fault activate during larger earthquakes. The northern limit of this microseismicity belt represents an approximation of the locking line of the Main Himalayan Thrust Fault.

[17] *Pandey et al.* [1999] suggest the presence of a “major transverse tectonic feature” in the area of the 20 August 1988 Udayapur earthquake. Earthquakes in this area line up in the NE-SW direction (Figure 8) and their depths are greater than 30 km, which suggest a hidden seismogenic structure beneath the Lesser Himalaya, clearly different from the Main Himalayan thrust. On the other hand, the Himalayan microseismicity belt shows a gap and an abrupt change in its azimuth between longitudes 87.3°E and 87.7°E (Figure 8). This gap lines up with the preferential orientation of the cluster in south Nepal (earthquakes in

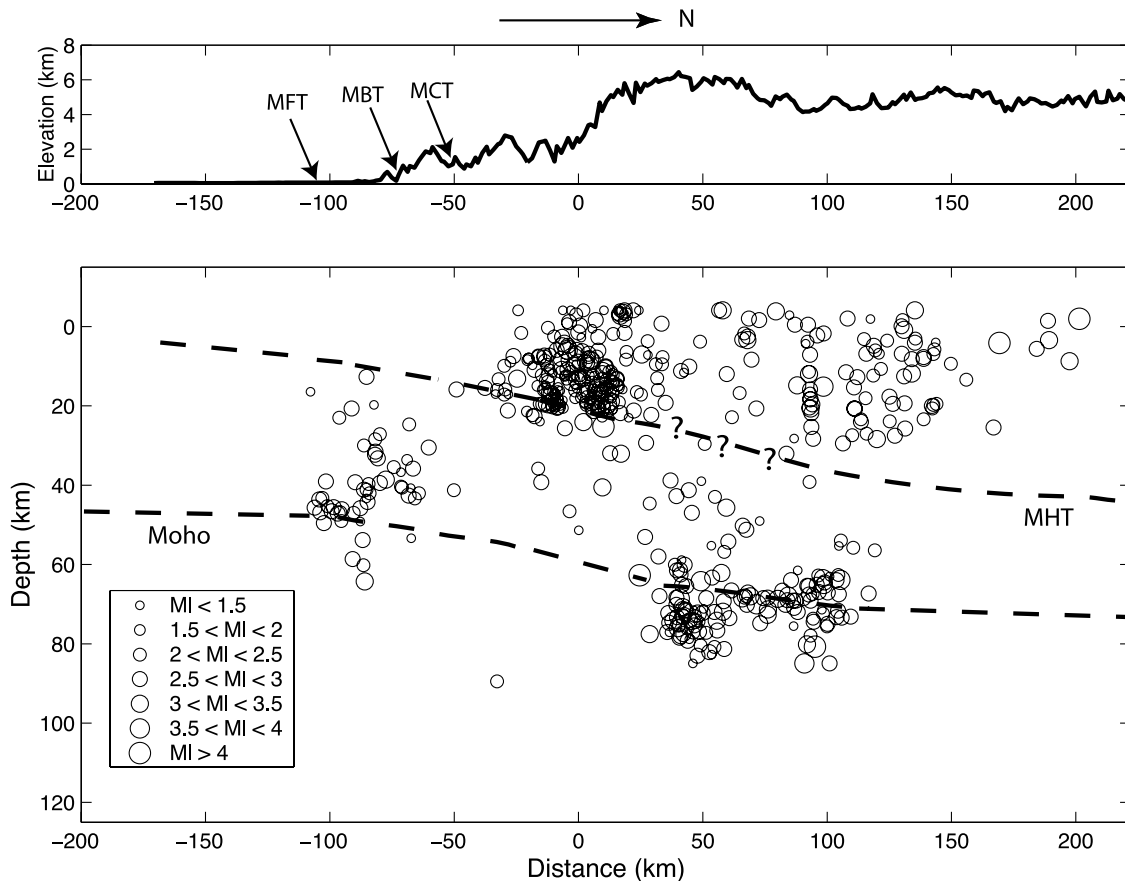


Figure 7. Event relocation in arc-normal cross section for the 542 earthquakes selected for inversion using VELEST. Topography at longitude 87°E is shown. Event symbol size is scaled by magnitude. Thick dashed lines show approximate locations of the Main Himalayan thrust fault (MHT) and the Moho, after *Schulte-Pelkum et al.* [2005]. Question marks are shown where receiver functions do not show a clear phase converter. MFT, Main frontal thrust; MBT, Main boundary thrust; MCT, Main Central Thrust.

the vicinity of the Udayapur earthquake). This transverse feature may mark the limit between different segments of the Main Himalayan Thrust Fault.

[18] The reader could argue that our picture of the seismicity in the study area is biased because we are using two 1-D velocity models to locate earthquakes in a region with an extremely complex tectonic configuration. For this reason, in Figures 10 and 11 we show relocations of the 542 events selected for the simultaneous inversion, when relocated using a 3-D tomographic velocity model [*Monsalve et al.*, 2005]. Even though locations of some earthquakes vary by a few kilometers, the main features that the seismicity reveals are consistent whether the events are located with 1-D velocity models or a 3-D velocity model. Thus, although our 1-D models are simple, their corresponding locations are sufficient to locate the seismicity and to constrain the earthquake depth.

7. Discussion: Upper Mantle Earthquakes Beneath the Himalayan Collision Zone?

[19] Teleseismic receiver functions, using data from the same seismic experiment described here [*Schulte-Pelkum et al.*, 2005], show clear P to S conversions from the Moho.

The approximate geometry and position of the Moho, the Main Himalayan Thrust (both from *Schulte-Pelkum et al.* [2005]), and the earthquakes (this study), all of them projected onto an arc-normal cross section, are shown in Figures 7, 9, and 11. Figure 9 shows that some events belonging to a cluster beneath the Lesser Himalaya of Nepal (near the Udayapur earthquake) are below the Moho and some events in south Tibet and beneath the High Himalaya are found at depths from 50 to 100 km below sea level. Histograms in Figure 12 show a bimodal distribution of earthquake depth with peaks in the upper crust (around 10 km below sea level) and near Moho depth (around 45 km for events south of 27.5°N and about 70 km for events north of that latitude). This contradicts the statement of *Mitra et al.* [2005] suggesting an absence of evidence of a bimodal depth distribution of earthquakes beneath the collision zone. It is difficult to ascertain whether all of the events around Moho depth are in the crust or in the mantle, but our purpose here is to demonstrate that at least some of them are in the upper mantle.

[20] In order to further test the mantle origin of some of these events and find the depth at which the misfit (RMS time residual) is minimum, we selected three high-quality deep earthquakes for a series of inversions for earthquake

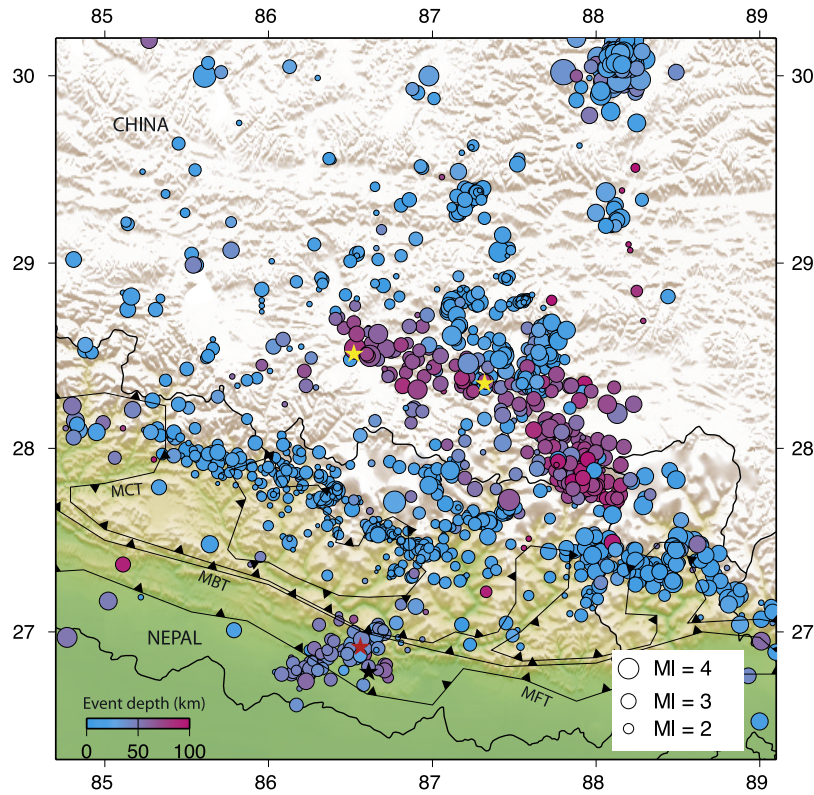


Figure 8. Map view of the whole set of earthquake events (1649) after refining the velocity model using VELEST. Symbols as in Figure 6. Black star marks the location of the Udayapur earthquake (20 August 1988). Yellow stars indicate location of earthquakes analyzed in Figures 13, 17, and 18. Red star gives the location of an earthquake referred in Figures 13, 15, and 16.

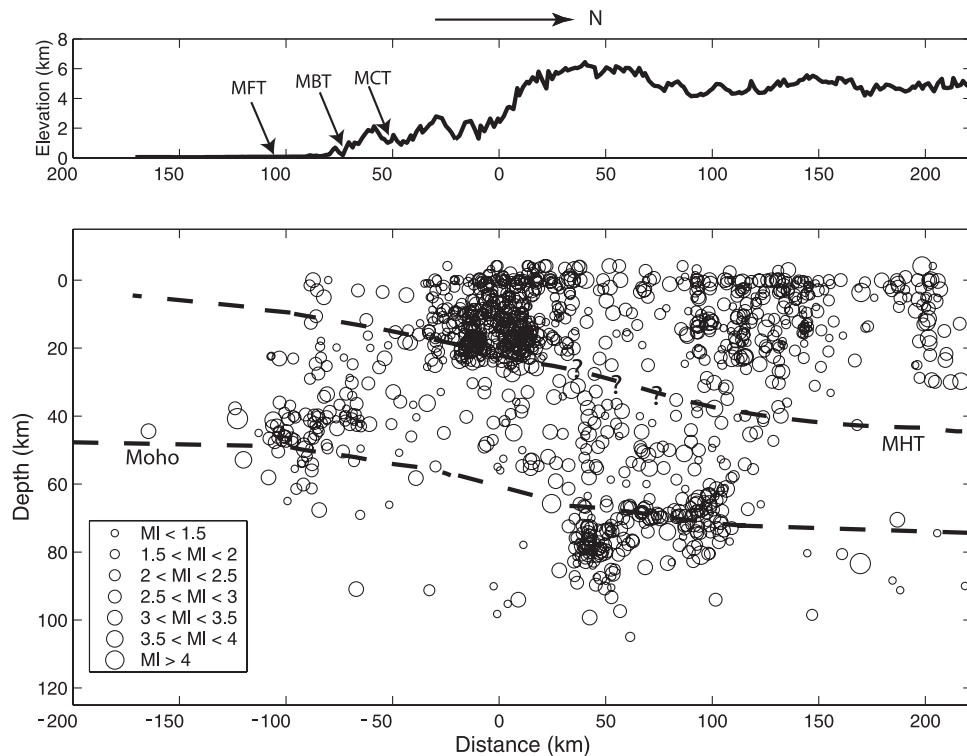


Figure 9. Locations of the whole set of earthquakes (1649) in Himalayan arc-normal projection. Topography and symbols are as in Figure 7.

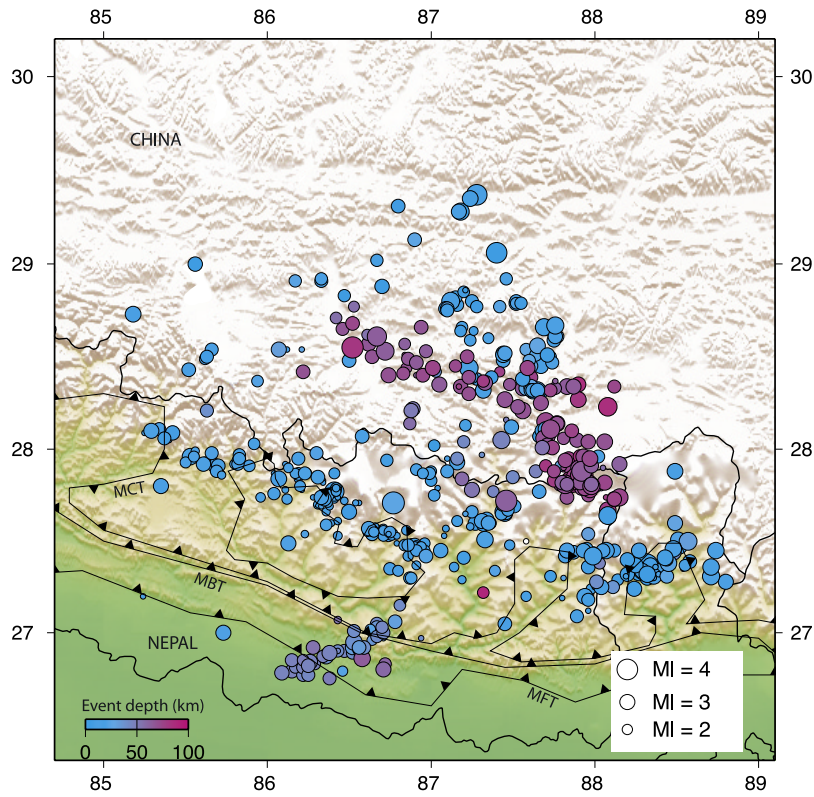


Figure 10. Map view of event relocations using a 3-D velocity model [from *Monsalve et al.*, 2005]. Only the subset of 542 events selected for inversion is shown. Symbols as in Figure 6.

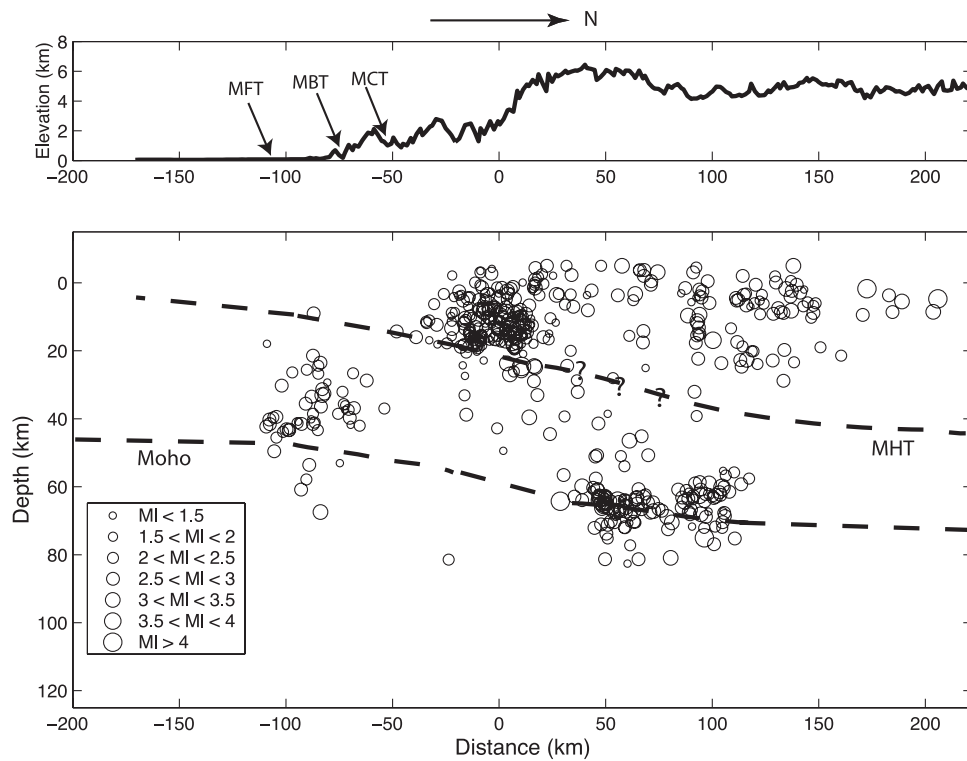


Figure 11. Himalayan arc-normal projection of event relocations using a 3-D velocity model [from *Monsalve et al.*, 2005]. Only the subset of 542 events selected for inversion is shown. Topography and symbols are as in Figure 7.

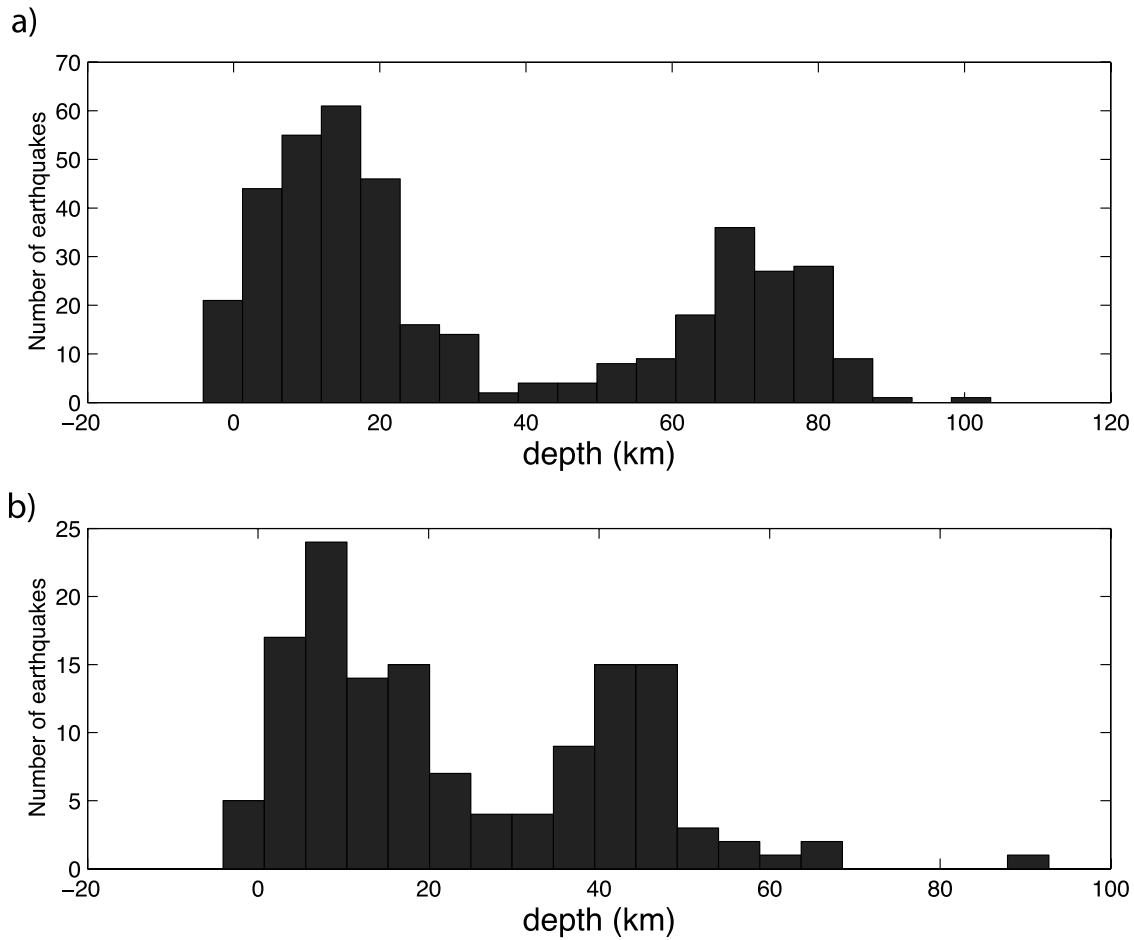


Figure 12. Histograms of earthquake depth. (a) Earthquakes north of 27.5°N. (b) Earthquakes south of 27.5°N. Note bimodal distribution of event depth. Histograms were made with the subset of 542 events used to invert for 1-D velocity structure.

location with fixed depth, so that only three parameters are free (latitude, longitude and origin time). A range of possible depths for each of the three earthquakes was tested. We used VELEST in the single event mode, with velocity models from Tables 4 and 5. Results for the three earthquakes marked by yellow and red stars in Figure 8 are shown in Figures 13 and 14, where the curves illustrate the variations of the RMS residual with depth for different subsets of arrivals. For the case of the two earthquakes in south Tibet, velocity models for both Nepal and Tibet were used because of their proximity to the boundary between the two regions (Figure 14).

[21] An event in south Nepal, in the vicinity of the Udayapur earthquake (red star on Figure 8), gives robust

evidence of being in the upper mantle: the minimum misfit is obtained at depths greater or equal than 63 km (Figure 13), which clearly correspond to the upper mantle at that location. This earthquake was located assuming a Moho depth of 55 km below sea level, which is a very conservative assumption when trying to demonstrate its mantle origin. *Schulte-Pelkum et al.* [2005] found that the Moho is shallower at the earthquake epicenter, with a depth below sea level between 40 and 50 km. A shallower than assumed Moho makes it even harder to place this earthquake in the crust unless an unrealistically slow crust is assumed. Figure 15 shows waveforms for this magnitude 3.15 event in south Nepal, with the observed arrival, the predicted arrival for the minimum misfit depth (67 km) and the

Table 4. Velocity Model for Nepal Obtained With VELEST^a

Depth Range, km	P Wave Speed, km/s	S Wave Speed, km/s
Surface to 3	5.5	3.2
3–23	5.7	3.2
23–55	6.3	3.7
>55	8.0	4.5

^aDepths are relative to sea level.

Table 5. Velocity Model for South Tibet Obtained With VELEST^a

Depth Range, km	P Wave Speed, km/s	S Wave Speed, km/s
Surface to 3	5.8	3.3
3–40	5.8	3.5
40–70	6.9	4.0
>70	8.6	4.9

^aDepths are relative to sea level.

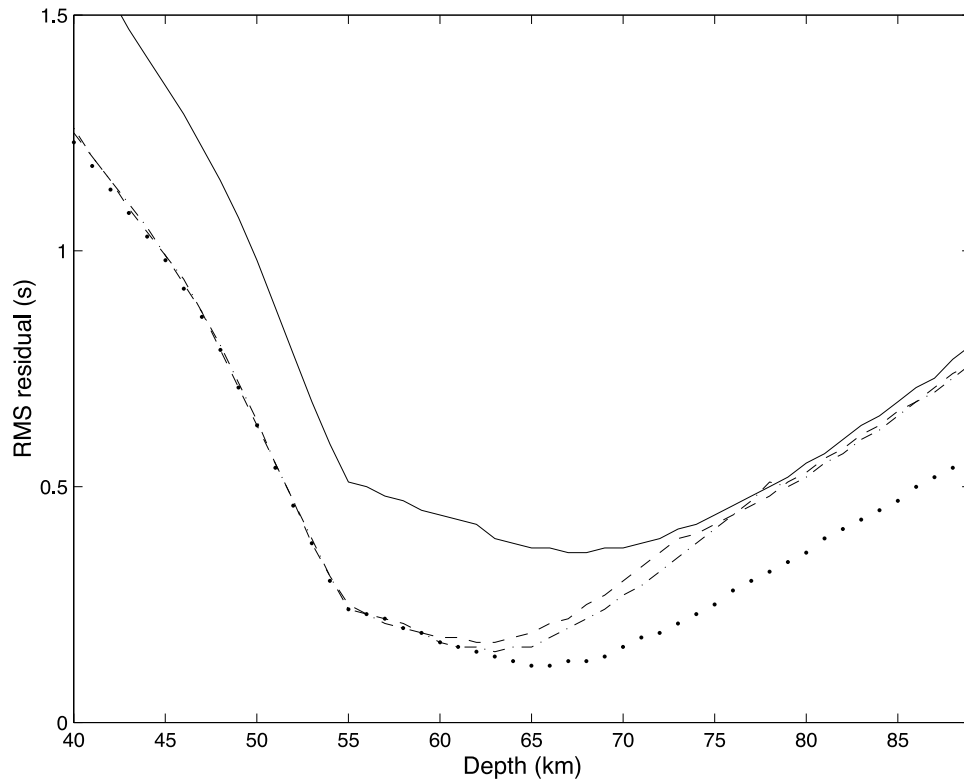


Figure 13. Plots of RMS versus depth for a possible upper mantle earthquake in south Nepal occurred on 16 July 2002 with a magnitude of 3.15 (latitude 26.86°N , longitude 86.58°E , denoted as a red star in Figure 8). Line styles indicate the subset of arrivals used for location. Solid line, all arrivals; dashed line, S arrivals at the three farthest stations are eliminated; dash-dotted line, P arrivals plus two first S arrivals; dotted line, P arrivals only.

predicted arrival for a lower crustal depth, after inverting all the available arrivals. When assuming a lower crustal depth for this earthquake, we fixed the depth to 48 km (the Moho is very unlikely to be more than 50 km deep at this latitude); Figure 15 shows that the predicted arrivals for a lower crustal hypocenter are several seconds apart (for most of the stations) from the observed arrivals. Figure 16 illustrates residuals at stations recording the earthquake for the cases of an upper mantle depth (Figures 16a and 16b) and a lower crustal depth (Figures 16c and 16d). It is clear from Figures 16c and 16d that the observed arrivals are late by several seconds with respect to the predicted ones for stations near the earthquake, and they are early for stations far from it, indicating that a depth of 48 km below sea level is too shallow. As Figures 15 and 16 suggest, the predicted arrivals for an event in the lower crust do not fit our observations.

[22] Depths of minimum misfit for the two selected earthquakes in south Tibet (yellow stars in Figure 8) are between 72 and 90 km below sea level (Figure 14), which correspond to upper mantle depths. However, the RMS versus depth function is very flat around the minimum (Figure 14). With the assumed geometries, it is possible that these earthquakes could be fitted in the crust if the speeds are different. Since speeds of the upper crust are well constrained given the earthquake and station distribution, a range of P wave speeds (between 6.3 and 7.4 km/s) for the

lower crust of south Tibet was tested, keeping the other parameters unchanged and using a V_p/V_s ratio of 1.73. Inversions for individual earthquake locations were performed while keeping the depth fixed. For each lower crustal velocity, we inverted for epicenter locations and origin times at 40 different depths (from 60 to 99 km) and chose the one with the minimum misfit (a procedure identical to the one we illustrate in Figures 13 and 14). Results are shown in Figure 17, where all the minimum misfit depths correspond to the upper mantle for both earthquakes (Figure 17a). Figure 17b shows that the largest values of RMS residuals are associated with the shallowest depths. In addition, we recalculated the Moho depth range below the earthquake epicenter by remigrating receiver functions to depth for each of the tested velocities. The error bars were defined by the depths at which the amplitude of the stacked receiver function reaches 5% of the amplitude of the direct P arrival. We found that earthquake depths are always greater than Moho depth, and are well outside the error bars of crustal thickness (Figure 17a). Caution should be exercised when comparing event and Moho depths from different studies, as the velocity models used for event location versus receiver function depth migration are likely different. Our comparison is internally consistent.

[23] Another possible way to fit these earthquakes in the crust would be having a deeper Moho. Therefore, using velocities from Table 5 and keeping the other boundaries

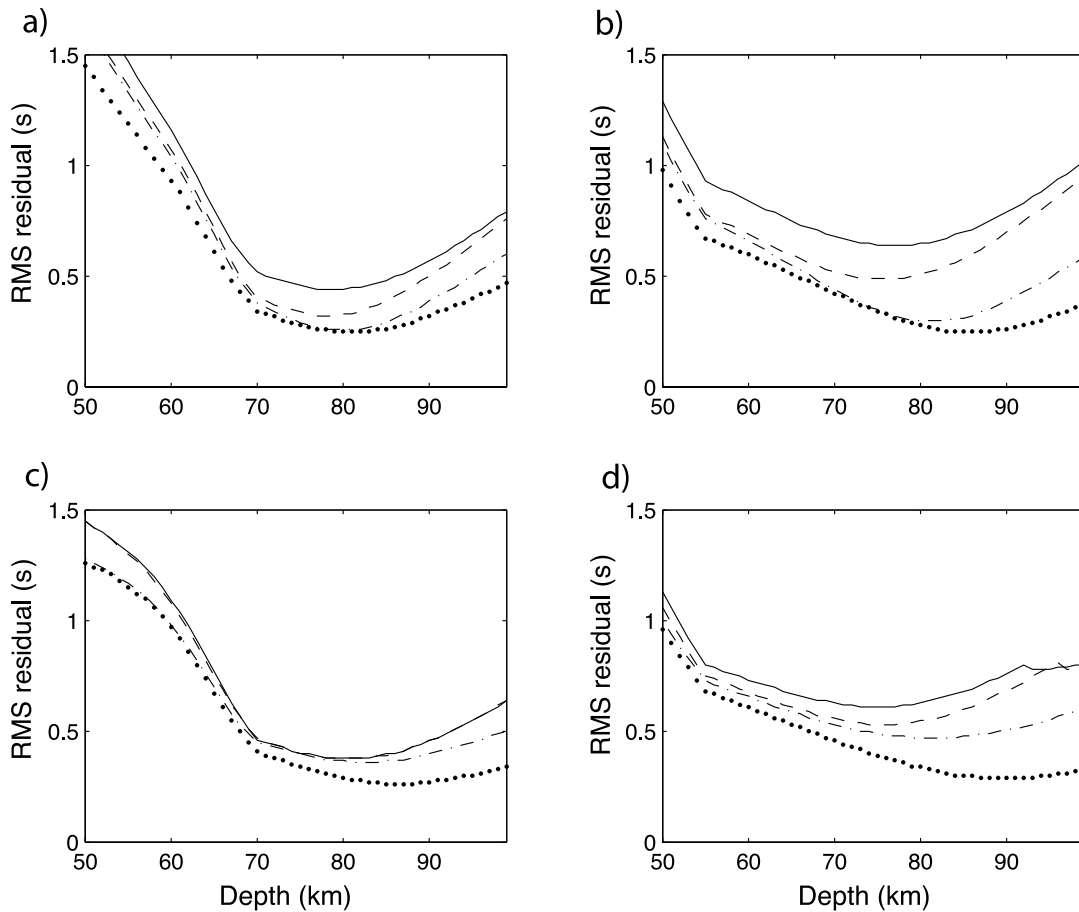


Figure 14. Plots of RMS versus depth for two possible upper mantle earthquakes in south Tibet (denoted as yellow stars in Figure 8). Line styles indicate the subset of arrivals used for location: solid lines, all arrivals; dashed lines, S arrivals at the five farthest stations are eliminated; dash-dotted lines, P arrivals plus two first S arrivals; dotted lines, P arrivals only. (a) The 8 May 2002 magnitude 4.17 earthquake in south Tibet (latitude 28.51°N , longitude 86.52°E) located with Tibet velocity model. (b) same as in Figure 14a but using Nepal velocity model. (c) The 25 October 2002 magnitude 2.45 earthquake in south Tibet (latitude 28.35°N , longitude 87.32°E) located with Tibet velocity model. (d) same as in Figure 14c but using Nepal velocity model.

unchanged, we found locations for this two events using Moho depths ranging from 60 to 90 km below sea level. We kept the earthquake depth fixed at every inversion. For each Moho depth, we also performed inversions at 40 different depths (from 60 to 99 km below sea level) and selected the one that represents the smallest RMS residual. For both earthquakes, we found that the Moho depth would have to be greater than 78 km for these events to be within the crust (Figure 18a); in addition, misfits are greater when the event is in the crust (Figure 18b). Experimenting with Moho depths and lower crustal velocities took us to the conclusion that the only way to fit these two earthquakes within the crust is to have a deeper Moho, at depths greater than about 78 km below sea level, which implies a crustal thickness greater than 83 km in the area of southern Tibet where these events are located. Receiver functions show that even for the case of a very fast crust (7.4 km/s in the lower crust), Moho depths below sea level are not likely to be greater than 72 km. So, even though these events might not be

much deeper than the Moho, an upper mantle location is the one that best fits the arrival time data and we conclude that a crustal source is unlikely.

[24] This evidence for brittle failure in the upper mantle is inconsistent with the hypothesis of *Jackson* [2002] that all the earthquakes in the continental lithosphere should locate in the crust. For more than 100 earthquakes beneath south Tibet and the Himalayas, an upper mantle location is the one that best fits the arrival time data. *Jackson* [2002] suggests that intermediate depth events beneath the Himalaya-Tibet system could be located at crustal depths, but this does not agree with our observations. *Maggi et al.* [2000b] also discuss deep earthquakes in this area and argue that if they are in the mantle, they should be associated with previously subducted oceanic lithosphere. Receiver function images [*Schulte-Pelkum et al.*, 2005] suggest that these earthquakes occur in Indian continental lithosphere underthrusting the High and the Tethyan Himalaya. The earthquake depths indicate that the levels of stress in some localized areas of

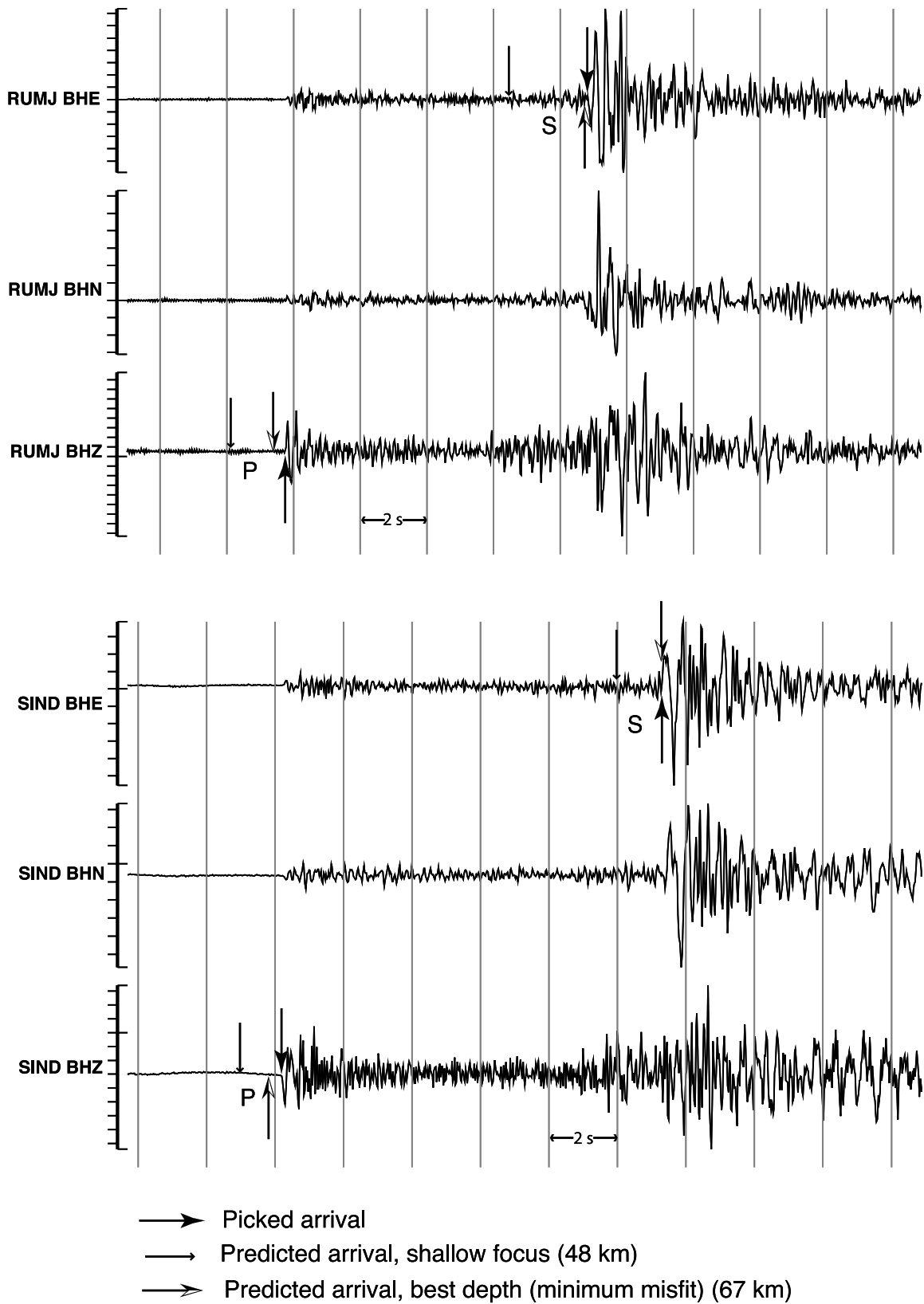


Figure 15. Waveforms for the magnitude 3.15 16 July 2002 earthquake in south Nepal (latitude 26.86°N, longitude 86.58°E, red star on Figure 8). Station code is on the left side of the seismograms. Lines with black and long arrowheads point at the picked arrival time. Lines with long and black/white arrowheads point at the predicted arrival time for the best depth (67 km in this case). Lines with short arrowheads point at the arrival time in the case the earthquake was 48 km deep. Amplitude scale is adjusted differently for each station.

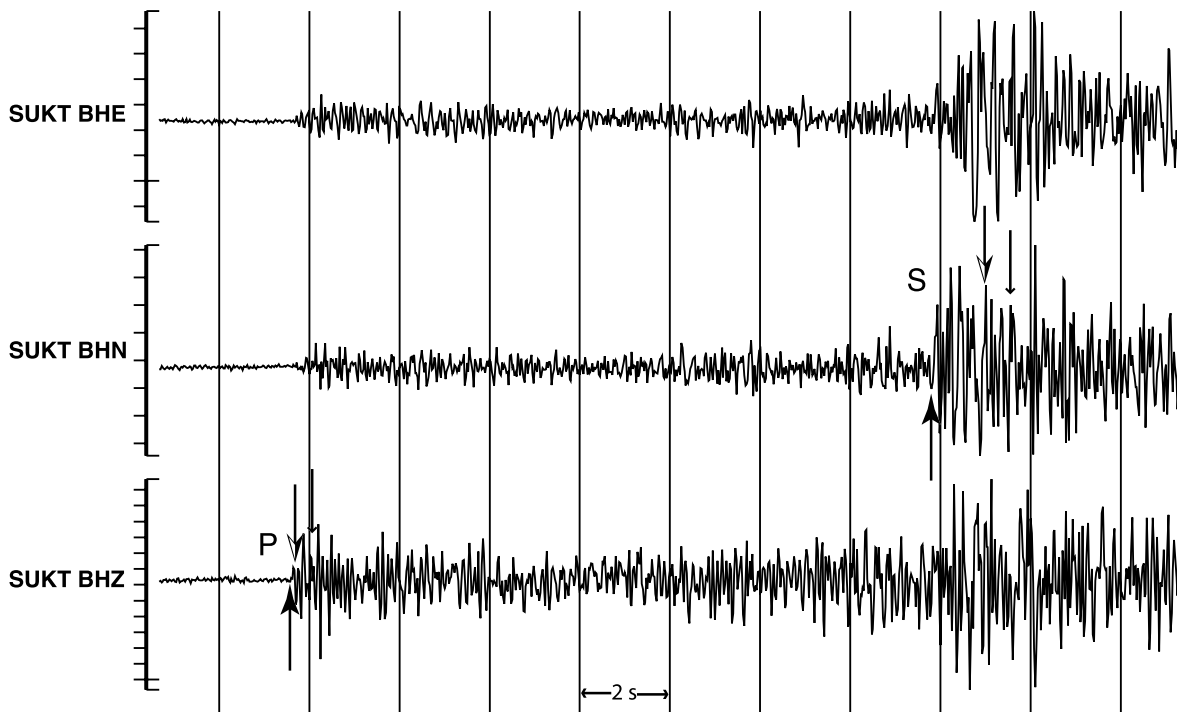
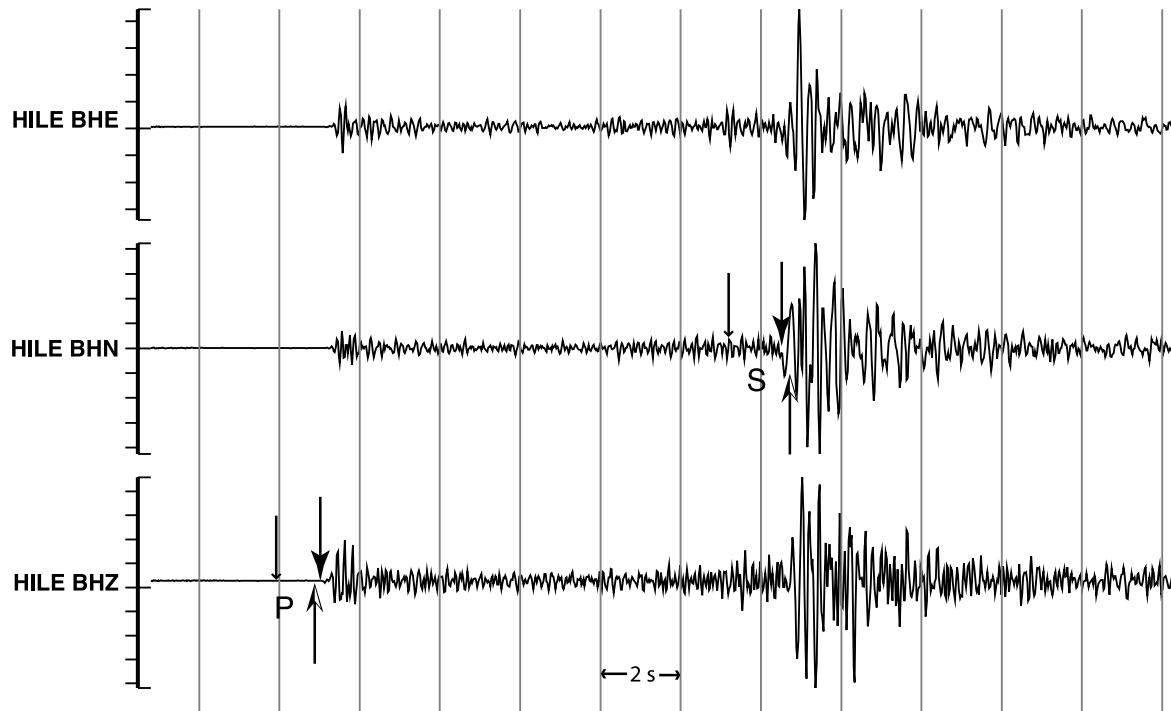


Figure 15. (continued)

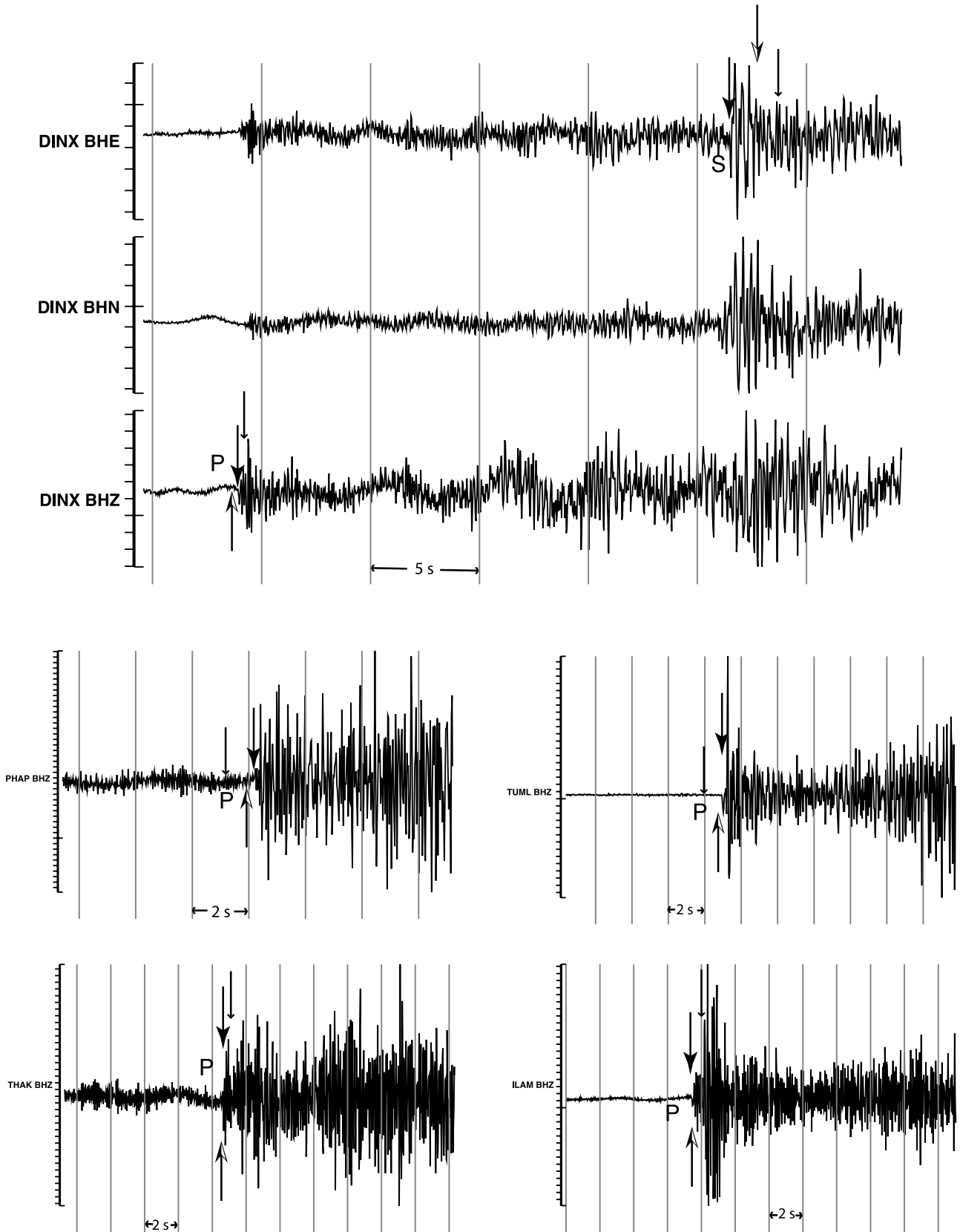


Figure 15. (continued)

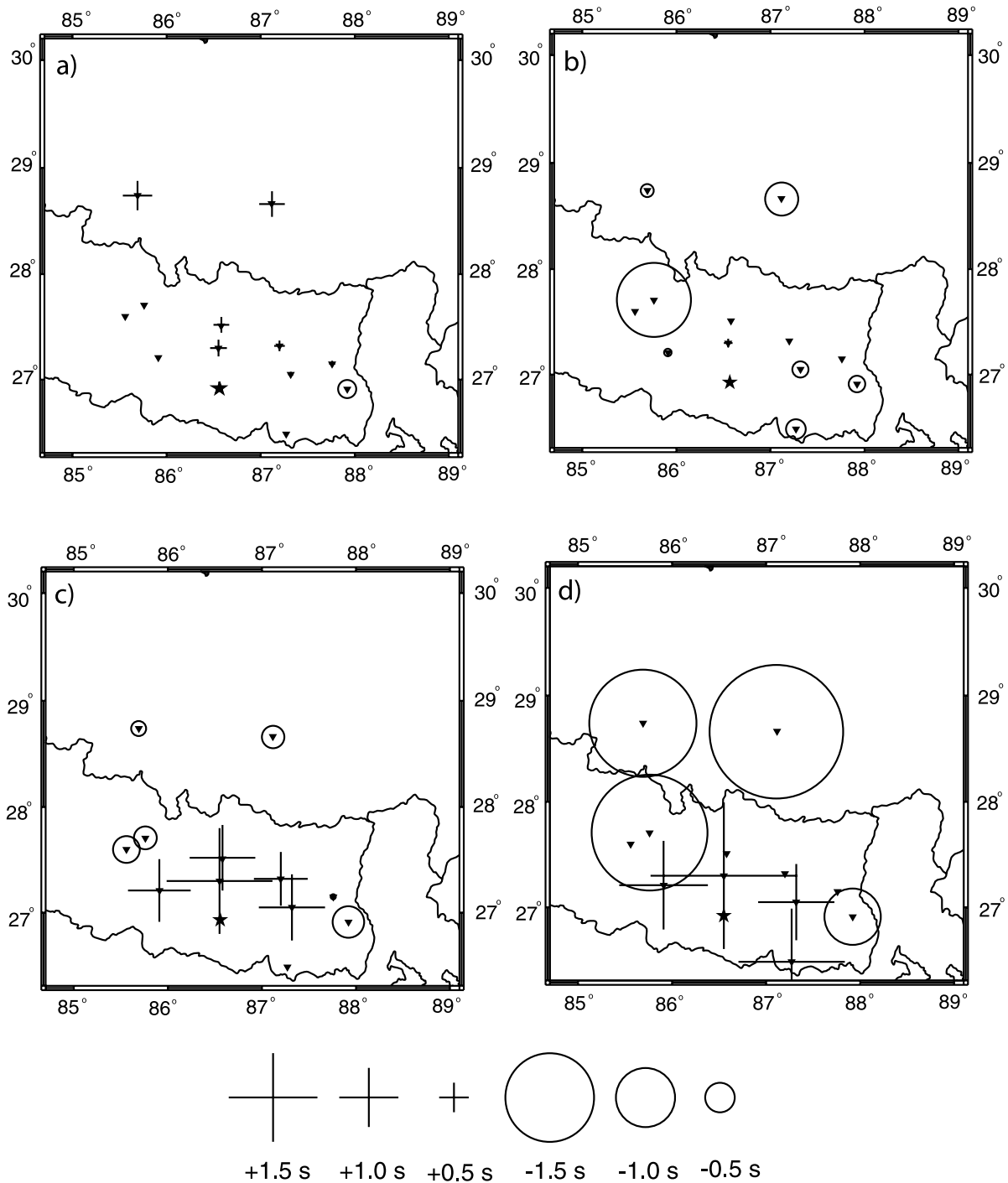


Figure 16. Maps of residuals at different stations for the magnitude 3.15 16 July 2002 earthquake in south Nepal (latitude 26.86°N, longitude 86.58°E, red star on Figure 8). Symbol sizes are scaled by the magnitude of the residual. Pluses indicate positive residuals (observed arrivals are late), and circles denote negative ones (observed arrivals are early). We only show stations with arrivals for this event. (a) Residuals for P arrivals at best fit depth. (b) Residuals for S arrivals at best fit depth. (c) Residuals for P arrivals at lower crust depth (48 km). (d) Residuals for S arrivals at lower crust depth (48 km).

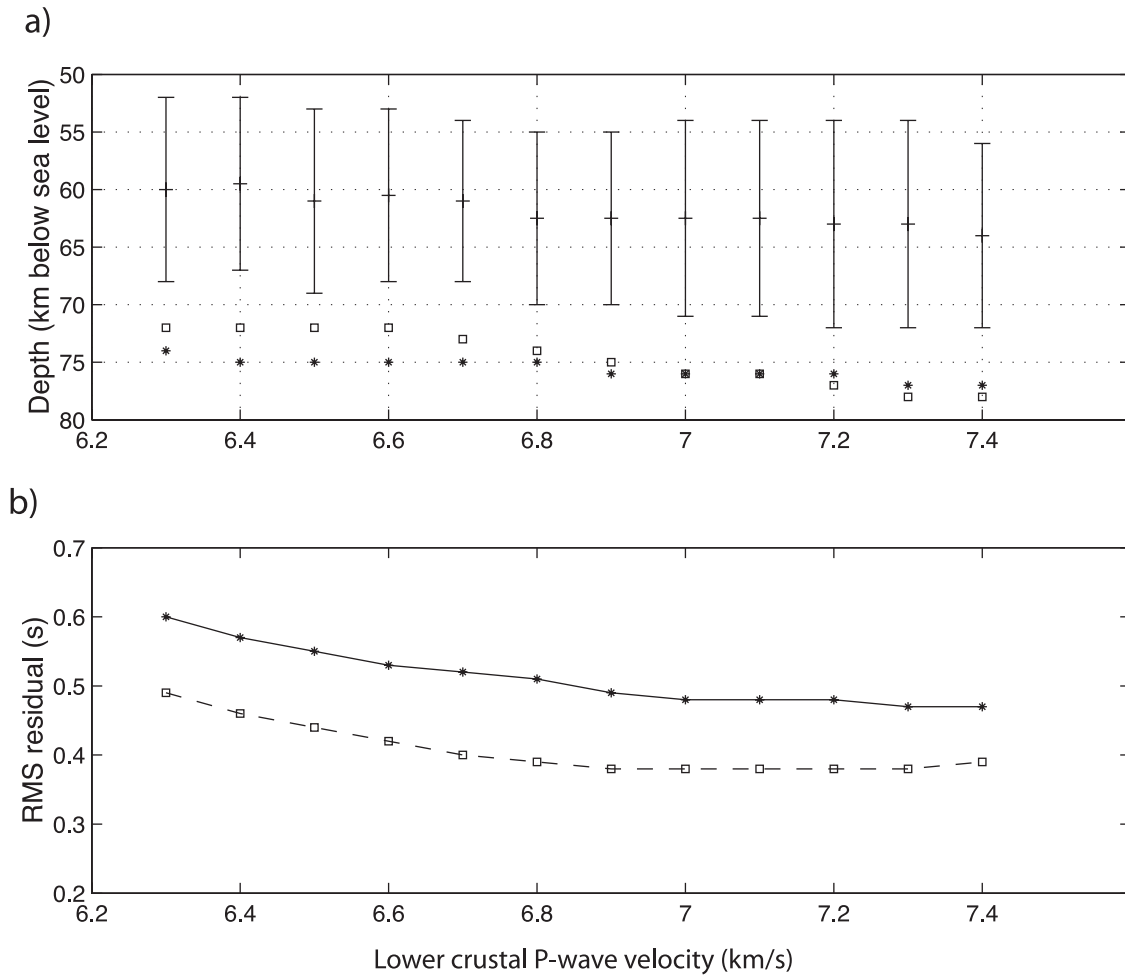


Figure 17. Results of earthquake location with different seismic velocities for the lower crust in south Tibet. Test was done for two earthquakes (yellow stars in Figure 8). Each inversion for earthquake location was performed keeping the depth fixed. We show depths for which the error is minimum for each lower crustal velocity. Asterisks, 8 May 2002 magnitude 4.17 event (latitude 28.51°N, longitude 86.52°E); squares, 25 October 2002 magnitude 2.45 earthquake (latitude 28.35°N, longitude 87.32°E). (a) Earthquake depth of minimum misfit versus P wave velocity of the lower layer (asterisks and squares). Vertical bars denote the range of possible depths for the Moho from receiver functions depth migrated with each velocity (see text for explanation). (b) RMS residual at best depth versus P wave velocity of the lower crust. See text for explanation.

the continental upper mantle are high enough to surpass the upper mantle brittle strength limits.

8. Conclusions

[25] The obtained seismicity (Figure 6) shows an alignment of microseismic events on the front of the High Himalaya, with most of the earthquakes being shallower than 25 km depth. In the Lesser Himalaya of Nepal there is a SW-NE oriented cluster of earthquakes at depths between 30 and 70 km in the 20 August 1988 Udayapur earthquake area. In southern Tibet we see clusters of crustal earthquakes and a NW oriented stripe of lower crust–upper mantle earthquakes in the 50–100 km depth range. Earthquakes along the Himalayan arc are scattered, and do not align in a single planar structure. Microseismicity during the inter-

seismic period occurs mainly in the hanging wall of the Main Himalayan Thrust. The spatial distribution of these small earthquakes is consistent with the presence of a crustal ramp. The geometry of the microseismicity belt along the topographic front of the High Himalaya suggests the presence of two different segments of the Main Himalayan Thrust Fault, with a boundary at longitudes ranging from 87.3°E to 87.7°E.

[26] The earthquakes beneath the study area in the Himalayan collision zone show a bimodal distribution with depth and the highest accumulation of events takes place in the upper crust and around the crust-mantle boundary depth. We found sufficient evidence that some of these earthquakes are in the upper mantle. At least one earthquake beneath the Lesser Himalaya of Nepal is indeed in the upper mantle. Depths of earthquakes near the Moho beneath southern

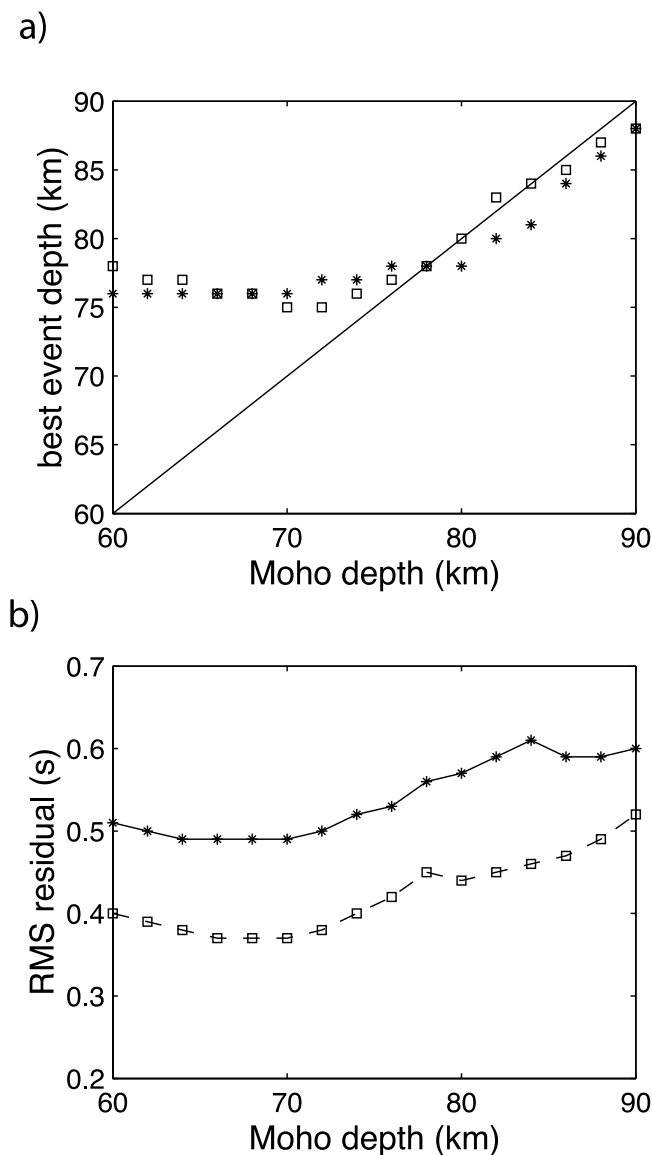


Figure 18. Results of earthquake location for different Moho depths in south Tibet. Test was done for two earthquakes (yellow stars in Figure 8). Each inversion for earthquake location was performed keeping the depth fixed. We show depths for which the error is minimum for each Moho depth. Velocity model as in Table 5, but with different Moho depth. Asterisks, 8 May 2002 magnitude 4.17 event (latitude 28.51°N , longitude 86.52°E); squares, 25 October 2002 magnitude 2.45 earthquake (latitude 28.35°N , longitude 87.32°E). (a) Earthquake depth of minimum misfit versus Moho depth. Solid line is used for reference and shows the case in which event depth equals Moho depth. (b) RMS residual at best depth versus Moho depth. See text for discussion.

Tibet have larger uncertainties, but the minimum misfits for reasonable crust models are attained for the cases in which these earthquakes are in the uppermost mantle. Receiver functions allow us to put constraints in the Moho depth that are internally consistent with the earthquake locations, and we found that the tested events are always below the Moho

and outside the error bar for its depth. According to the arrival times of earthquakes beneath the HIMNT array, over a hundred intermediate depth earthquakes are at sub-Moho depth, which indicates that the upper mantle in the continental lithosphere in some localized areas deforms by brittle processes.

[27] **Acknowledgments.** We thank Peter Molnar and Craig Jones for their constant advice and suggestions during this study. We thank Frederick Blume for all his work on building the database and Charlotte Rowe for her assistance on the use of VELEST. We also thank the Department of Mines and Geology of Nepal and the Chinese Academy of Science for their assistance with the HIMNT field project. This material is based on work supported by National Science Foundation grant 9903066.

References

- Chen, W., and P. Molnar (1983), Focal depths of intracontinental and intraplate earthquakes and their implications for the thermal and mechanical properties of the lithosphere, *J. Geophys. Res.*, *88*, 4183–4214.
- Chen, W., and Z. Yang (2004), Earthquakes beneath the Himalayas and Tibet: Evidence for strong lithospheric mantle, *Science*, *304*, 1949–1952.
- Chen, W., J. Nabelek, T. Fitch, and P. Molnar (1981), An intermediate depth earthquake beneath Tibet: Source characteristics of the event of September 14, 1976, *J. Geophys. Res.*, *86*, 2863–2876.
- Cotte, N., H. Pedersen, M. Campillo, J. Mars, J. Ni, R. Kind, E. Sandvol, and W. Zhao (1999), Determination of the crustal structure in Southern Tibet by dispersion and amplitude analysis of Rayleigh waves, *Geophys. J. Int.*, *138*, 809–819.
- Dasgupta, S., et al. (2000), *Seismogenic Atlas of India and Its Environs*, Geol. Surv. of India, Kolkata.
- de la Torre, T., and A. Sheehan (2005), Broadband seismic noise analysis of the Himalayan Nepal Tibet seismic experiment, *Bull. Seismol. Soc. Am.*, *95*, 1202–1208.
- de la Torre, T., G. Monsalve, and A. Sheehan (2005), Focal mechanisms from moment tensor solutions and first-motion polarities of shallow to deep local earthquakes in eastern Nepal and southern Tibet, paper presented at SSA Annual Meeting, Incline Village, Nev., 27–29 April.
- Galvé, A., M. Sapin, A. Hirn, J. Diaz, J.-C. Lpigne, M. Laigle, J. Gallart, and M. Jiang (2002), Complex images of Moho and variation of V_p/V_s across the Himalaya and South Tibet, from a joint receiver-function and wide-angle-reflection approach, *Geophys. Res. Lett.*, *29*(24), 2182, doi:10.1029/2002GL015611.
- Jackson, J. (2002), Strength of the continental lithosphere: Time to abandon the jelly sandwich?, *GSA Today*, *12*, 4–10.
- Jouanne, F., J. Mugnier, J. Gamond, P. LeFort, M. Pandey, L. Bollinger, M. Flouzat, and J. Avouac (2004), Current shortening across the Himalayas of Nepal, *Geophys. J. Int.*, *157*(1), doi:10.1111/j.1365-246X.2004.02180.
- Kayal, J. (2001), Microearthquake activity in some parts of the Himalaya and the tectonic model, *Tectonophysics*, *339*, 331–351.
- Kissling, E., W. Ellsworth, D. Eberhart-Phillips, and U. Kradofler (1994), Initial reference models in local earthquake tomography, *J. Geophys. Res.*, *99*, 19,635–19,646.
- Langin, W., L. Brown, and E. Sandvol (2003), Seismicity in central Tibet from project INDEPTH III seismic recordings, *Bull. Seismol. Soc. Am.*, *93*, 2146–2159.
- Lave, J., and J. Avouac (2000), Active folding of fluvial terraces across the Siwaliks Hills, Himalayas of central Nepal, *J. Geophys. Res.*, *105*, 5735–5770.
- Maggi, A., J. Jackson, D. McKenzie, and K. Priestley (2000a), Earthquake focal depths, Effective elastic thickness and the strength of the continental lithosphere, *Geology*, *28*, 495–498.
- Maggi, A., J. Jackson, K. Priestley, and C. Baker (2000b), A reassessment of focal depth distributions in Southern Iran, the Tien Shan and northern India: Do earthquakes really occur in the continental mantle?, *Geophys. J. Int.*, *143*, 629–661.
- Mitra, S., K. Priestley, A. Bhattacharyya, and V. Gaur (2005), Crustal structure and earthquake focal depths beneath northeastern India and southern Tibet, *Geophys. J. Int.*, *160*, 227–248.
- Molnar, P., and W. Chen (1983), Focal depths and fault plane solutions of earthquakes under the Tibetan Plateau, *J. Geophys. Res.*, *88*, 1180–1196.
- Monsalve, G., A. Sheehan, and C. Rowe (2005), Seismicity and 3-D velocity structure of the Himalayan Collision Zone: Lateral variations in lithospheric structure, *Eos Trans., AGU*, *86*(52), Fall Meet. Suppl., Abstract T52A-07.
- Nelson, K. (1996), Partially molten middle crust beneath southern Tibet: Synthesis of project INDEPTH results, *Science*, *274*, 1684–1688.

- Ni, J., and M. Barazangi (1984), Seismotectonics of the Himalayan collision zone D Geometry of the underthrusting Indian Plate beneath the Himalaya, *J. Geophys. Res.*, *89*, 1147–1163.
- Pandey, M., R. Tandukar, J. Avouac, J. Lave, and J. Massot (1995), Interseismic strain accumulation on the Himalayan crustal ramp (Nepal), *Geophys. Res. Lett.*, *22*, 751–754.
- Pandey, M., R. Tandukar, J. Avouac, J. Vergne, and T. Heritier (1999), Seismotectonics of the Nepal Himalaya from a local seismic network, *J. Asian Earth Sci.*, *17*, 703–712.
- Pavlis, G., F. Vernon, D. Harvey, and D. Quinlan (2004), The generalized earthquake-location (GENLOC) package: An earthquake location library, *Comput. Geosci.*, *30*, 1079–1091.
- Sapin, M., X. Wang, A. Hirn, and Z. Xu (1985), A seismic sounding in the crust of the Lhasa block, Tibet, *Ann. Geophys.*, *3*, 637–646.
- Schulte-Pelkum, V., G. Monsalve, A. Sheehan, M. Pandey, S. Sapkota, and R. Bilham (2005), Imaging the Indian subcontinent beneath the Himalaya, *Nature*, *435*, 1222–1225.
- Zhao, L., and D. Helmberger (1991), Geophysical implications from relocations of Tibetan earthquakes: Hot lithosphere, *Geophys. Res. Lett.*, *18*, 2205–2208.
- Zhu, L., and D. Helmberger (1996), Intermediate depth earthquakes beneath the India-Tibet collision zone, *Geophys. Res. Lett.*, *23*, 435–438.

G. Monsalve, V. Schulte-Pelkum, and A. Sheehan, Department of Geological Sciences, University of Colorado, 2200 Colorado Avenue, Boulder, CO 80309-0399, USA. (monsalve@colorado.edu)

M. R. Pandey and S. Rajaure, Department of Mines and Geology, National Seismological Centre, Lainchaur, Kathmandu, Nepal.

F. Wu, Department of Geological Sciences and Environmental Studies, State University of New York at Binghamton, P.O. Box 6000, Binghamton, NY 13902-6000, USA.